Received: 22 February 2023 | Accepted: 3 March 2023

DOI: 10.1002/mawe.202300020

ARTICLE

WILEY VCH

Using 3D-scanners and finite element method to assess the fatigue life of welded joints based on the actual geometry of seam welds: realistic modelling of notches at the weld toe

Verwendung von 3D-Scannern und Finite Elemente Methode zur Berechnung der Ermüdungsfestigkeit von Schweißnähten anhand der realen Geometrie: Modellierung der Nahtübergangskerben

R. Späth | M. Steinebrunner

Universität der Bundeswehr München, Fakultät für Maschinenbau, Neubiberg, Germany

Correspondence
R. Späth, Universität der Bundeswehr München, Fakultät für Maschinenbau, Neubiberg, Germany.
Email: ralf.spaeth@unibw.de

Abstract

To predict the service life of welded joints, the seam welds of samples (cross joint, K-seam, sheet thickness 15 mm and a laser-welded butt joint, sheet thickness 6 mm, both made of steel quality S 355) are recorded using a 3D scanner. The data obtained in this way is processed and transferred to a finite element method program. The meshing of the weld seams is very detailed. A finite-element-method stress calculation is then carried out. The real samples are tested in a fatigue test up to the point of cracking. The results from calculation and test are then compared. A possible crack location can be predicted very well using the finite element method results. The cracks in the real test are always in the area of very high or often the absolute highest calculated stresses. A prediction of the service life in the fatigue test is possible with a certain scatter – close to the usual scatter for welded joints. Based on the results of 19 samples, a fatigue class for local stress (based on the real geometry) of FAT 300 can be preliminary estimated for the cross-joint specimens. Definition according to the specifications of the International Institute of Welding (FAT at 2 mio. cycles, survival probability 97.7%).

KEYWORDS
3D-scan, fatigue assessment, fatigue test, finite element method, welded joints

Abstract

Zur Bestimmung der Lebensdauer von Schweißnähten, wurden

Schweißproben (Kreuzstoß, K-Naht, Blechdicke 15 mm und laserstahlgeschweißt: Stumpfstoß, Blechdicke 6 mm, beide aus S 355-Baustahl) mittels 3D-Scanner digitalisiert. Die dadurch erhaltenen Daten wurden verarbeitet und in ein Finite-Elemente-Methode-Programm übertragen. Die Vernetzung wurde dabei sehr fein gewählt. Daran anschließend erfolgte die Berechnung der Elementspannungen. Die ausgeführten Proben wurde bis zum Rissbeginn mittels Schwingversuch getestet. Die Ergebnisse wurden dann miteinander verglichen. Mögliche Versagensorte konnten mit den Finite-Elemente-Methode-Ergebnissen gut vorhergesagt werden. Risse in der echten Probe traten immer in Regionen mit sehr hohen und oft auch mit den höchsten errechneten Spannungen auf. Eine Aussage zur Lebensdauer ist mit entsprechender Streuung (ähnlich der üblichen Streuung bei Schweißproben) möglich. Anhand von 19 Proben konnte auf Basis der Realgeometrie für die lokalen Spannungen der Kreuzproben eine vorläufige Schwingfestigkeitsklasse gemäß dem International Institute of Welding (2 Mio. Zyklen und einer Überlebenswahrscheinlichkeit von 97,7 %) von FAT-300 abgeschätzt werden.

SCHLÜSSELWÖRTER
3D-Scan, Ermüdungsfestigkeit, Finite-Elemente-Methode, Schweißnähte, Schwingversuch

1 | INTRODUCTION

In addition to other factors (metallurgy, residual stresses, etc.), the fatigue strength of welded joints is very strongly influenced by the geometric notch effect. In the case of welds with full penetration, the geometry of the surface is of great importance. Different methods have been developed for calculating the fatigue strength of weld seams, which are now in general use [1]. A major challenge in finite element modelling of welds is the great variability of the real seam surface. Various methods have been developed to generate abstract models from a theoretical seam geometry (according to the drawing). The main problem here is the modelling of the sharp transitions at the weld toe and root. As a solution, an approach with a standardized radius has been pursued for a long time [2]. This makes it easy to model even complex seams in detail. For different seam shapes and sheet thicknesses various FAT-classes are published in [3]. With these methods the real seam geometry has not been modelled. The whole process of scanning and finite element-modelling of real welds has become much more accomplishable due to the dramatically increased performance of computer technology and effective recording of real geometries by scanning systems. In this article, the possibilities and limits of the finite element calculation of digitized real geometries of welded joints are shown. This is done using two examples: Gas metal arc welded cross joint, sheet thickness 15 mm (K-seam with full penetration welding) and a laser-welded butt joint, sheet thickness 6 mm (carbon dioxide laser). Both types are made of standard structural steel of quality class S 355 and were subjected to fatigue testing after the calculation steps (digitization of the real geometry, transfer to the finite element method program, modelling and stress analysis). A comparison of the test results with the calculations follows.

2 | STATE OF THE ART

The strength behaviour of welded joints has been dealt with in many publications, standards and regulations. In most cases, no real or only an idealized seam shape is assumed. The strength is often determined on the basis of nominal or structural stresses: the locally resulting stress peaks in the real weld seam are hardly recorded and usually considered by coefficients or notch factors. This is consistent and practical, e.g., stored in the catalogue of FAT classes (International Institute of Welding, fatigue analysis) [1]. Approaches also considering the local stress increase can be found in a standardized but idealized method of extrapolation using so-called structural stresses. Here, the stress is determined at two or more defined distances from the weld seam (e.g., metrologically using strain gauge chains or mathematically using finite elements) and then extrapolated to the weld toe [1]. Local tensions e.g., in a sharp notch of a seam

transition can hardly be determined metrologically: The application of strain gages over an edge is not advantageous. In the mathematical stress analysis with idealized seam transitions, there are also large uncertainties when evaluating the numerical results at a point of discontinuity (=sharp edge). To determine the local stresses of a real weld seam, it is essential to record the real geometry. Thanks to developments in the 3D acquisition of surfaces, it is now possible to optically scan and digitize any geometrically undefined surface. A closed volume is then generated from the point clouds determined in this way, which then serves as the basis for structural calculations using the finite element method. This method has already been used in published projects, often with the aim of generating notch stress Wöhler curves for idealized seam models [4–7]. The present work shows that the method is directly suitable for the evaluation of seam welded joints and a fatigue-class according to the International Institute of Welding (IIW) recommendations is proposed. In the not-too-distant future, critical seams may also be evaluated on an industrial scale. The main drivers here are a further significant increase in computing power. In addition, it should be shown whether a non-linear material modelling in the calculation significantly increases the validity of the results.

3 | SPECIMEN AND EXPERIMENTAL DETAILS

Two different specimen types were examined (both made of structural steel of strength class S 355): Metal activ gas-welded cruciform joint, sheet thickness 15 mm (K-seam with full penetration, PA 135), Figure 1. Of the nineteen samples examined, five were subjected to annealing to reduce residual stresses. The fatigue tests showed no statistically reliable differences to the non-annealed samples. The other samples are laser-welded butt joint, sheet thickness 6 mm, 4 pieces, Figure 2. All four samples were subjected to an annealing treatment to reduce residual stresses.

The seam geometry is recorded here with a so-called structured light scanner. In contrast to a laser scanner, a large measuring volume can be recorded very quickly. A grid of strips with a variable width is projected onto the object for image acquisition. The resulting images are captured with a second lens. Typical capture time is approximately 1 second per view. The object can be placed on a special rotating device for capturing it from different angles. This is linked to the recording software and thus allows an automated process. The rotation steps can be set completely freely (e.g., 20 steps over 360°). Since the turntable transmits the position to the software, each further measurement can be aligned automatically. This means that many measurements are possible without intervention. With the existing device, the described recording of the surface takes place with a minimum point spacing of 18 μm (this depends on the selected pair of lenses). Since several measurements are usually superimposed, the detail resolution of several measurements is higher but cannot be precisely quantified: How the points of several measurements are distributed on the object cannot be predicted. The distribution of the measured points using 13 rotational steps with the turntable is higher than by using rotational 27 steps, Figure 3. A

FIGURE 1 Cruciform joint: sheets 15 mm thick, metal active gas welding PA 135, K-seam with full penetration welding, samples provided by industry partners.

BILD 1 Kreuzstoß: 15 mm Blechstärke, MAG Schweiwßung, PA 135, K-Naht mit voller Durchschweißung, Proben durch Industriepartner gestellt.

defined precision cannot be given, as the distribution shows a statistical behavior.

For optimal detection, it is absolutely necessary that the surface of the measurement object does not shine, but appears matt. Applying a white developer spray, as known from crack detection using dye penetrant methods, proved to be suitable. Narrow and deep openings, such as bores, cracks, etc. cannot be detected with this method. The 3D data of the measurement object recorded in this way are point clouds within the scanners coordinate system. Before further processing, the measuring points must be triangulated to form surfaces. A volume for modelling with finite element methods can then be generated. The steps briefly mentioned here are quite complex in terms of data technology and can be accomplished with various software packages. To model a calculable finite element, model several processual steps have to be made, Figure 4. The partial image on the left shows the photo of the real sample. The right sub-image shows a pictorial representation of the measured points; this is not a photo.

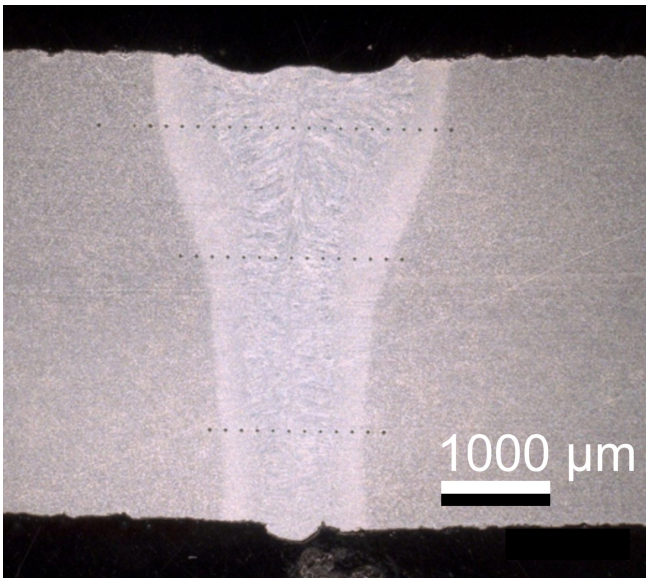

FIGURE 2 Specimen type with laser-welded butt joint, sheet thickness 6 mm, cross-section of the seam; samples provided by Fraunhofer IWS.

BILD 2 Prüfling mit geschweißter Stumpfnaht, Blechstärke 6 mm, Schnitt der Naht, Proben durch Fraunhofer IWS gestellt.

The meshing fineness to reliably represent the geometry is very high, Figure 5. In preliminary studies this was examined for various weld seam shapes. Networking with the theoretically very precise hexahedron elements is not easily possible with the geometry presented here. Therefore, tetrahedron elements are used for meshing. For calculation results that are as precise as possible, however, second-order elements must be used (in the model shown, these are almost 8.3 million elements). The number of degrees of freedom in the calculation is approx. 35 million. The load case of the real fatigue test is easy to apply in the model (load amplitude). The results are shown in the next section. With the method presented, only

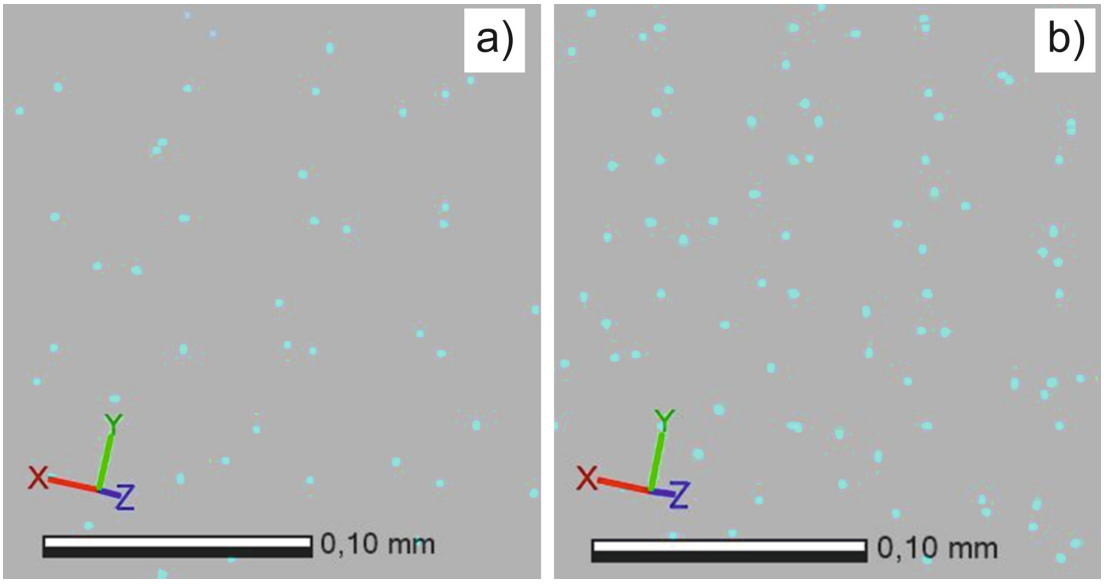

FIGURE 3 Distribution of measured points when scanning the same sample with a different number of shots: a) 13 shots (also rotational steps of the turning device) b) 27 shots. The distribution is denser, but still scattered.

BILD 3 Verteilung der Messpunkte bei Scanverfahren mit unterschiedlicher Anzahl von Aufnahmen: a) 13 Aufnahmen (entspricht auch der Anzahl der Schritte des Drehtisches) b) 27 Aufnahmen. Die Verteilung ist dichter, aber immer noch mit einer Streuung versehen.

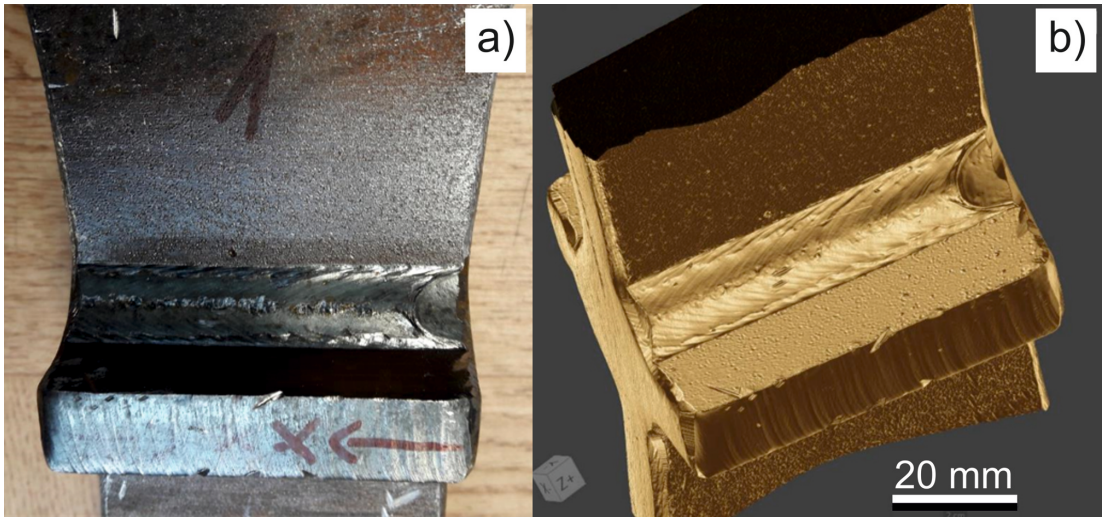

FIGURE 4 Pictorial sequence of two processing steps: a) Real sample b) pictorial representation of the measured points (no photo).

BILD 4 Darstellung von zwei Prozessschritten: a) Reale Probe b) Bildliche Darstellung der erfassten Punkte (kein Foto).

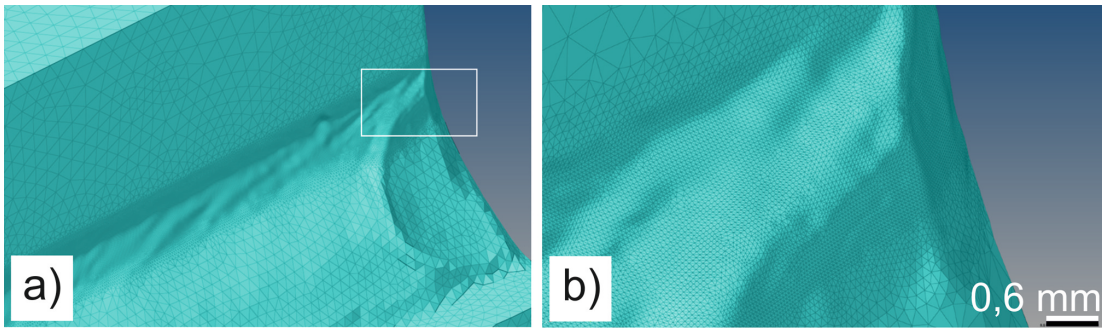

FIGURE 5 a) detail of the extremely fine mesh; b) further enlargement of the framed section from the left partial image. Minimum size of the finite elements approx. 40 μm.

BILD 5 a) Ausschnitt der extrem feinen Vernetzung; b) Detailvergrößerung des Rechteckbereichs aus dem linken Teilbild. Minimale Elementgröße ca. 40 μm.

the outer geometric notches can be detected. For a realistic classification of the results, it should be noted that some aspects are not considered in this procedure:

- Internal errors, e.g., root of fillet welds, lack of fusion, pores, inclusions etc.
- Cracks or crack-like notches on the surface
- Influences from residual stresses
- Metallurgical peculiarities (local hardening, special structural formation, etc.)

4 | RESULTS FROM CALCULATION AND EXPERIMENT

The samples were calculated using the finite element method and then tested by using a high-frequency pulsator. The stress level was chosen in a way that a service life in the medium fatigue strength range can be expected. The position and level of the maximum stresses correlate well with the test results, Figure 6.

The laser butt weld shows the two transitions at the weld toe on the front side of the seam and on the root side. The highest stress peaks at the transition from the root to the base material, Figure 7. For all laser-welded specimens, the highest calculated stress were calculated for the root side at the transition from the root to the base material. As a result of the fatigue tests, the cracks were only found at these points.

5 | DISCUSSION OF THE RESULTS

This allows the following statements to be made with regard to the location of failure and the service life:

In all samples, the crack in the fatigue test occurred in the very high stressed area of the finite element method calculations. However, it was not always the case that the point with the absolute highest calculated stress was also the location of the crack origin. In the real test, the crack was partly located at locations that were slightly below the maximum stress in the calculation, but still close to it. An absolutely certain statement that the sample will fail at specific points is not possible. However, critical areas can be located with pinpoint accuracy.

It is not yet possible to predict the exact service life of the samples in the fatigue test - the scatter of the failure causes and processes is too large. On the basis of the stresses calculated using finite element method, however, service life ranges can be calculated with a certain scatter, Figure 8. The stresses calculated using finite element method are plotted against the number of cracking load cycles determined in the fatigue test. Using the definition of the FAT-classes according to the IIW (FAT-class is the stress range in MPa at 2 Mio.

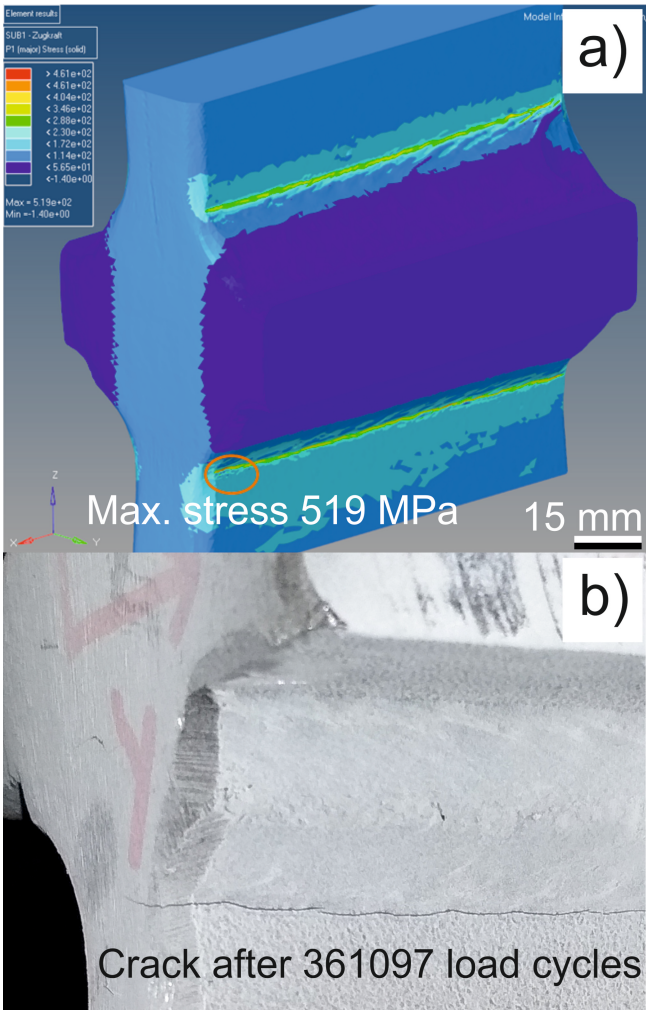

FIGURE 6 Result of the calculated cross joints: a) Contour plot of the 1st principal stress; b) crack position at the same point in the fatigue test after 361,097 load cycles.

BILD 6 Rechenergebnis für eine Kreuzprobe: a) Verteilung der 1. Hauptspannung; b) Position des Risses am gleichen Ort nach Schwingversuch mit 361.097 Lastspielen.

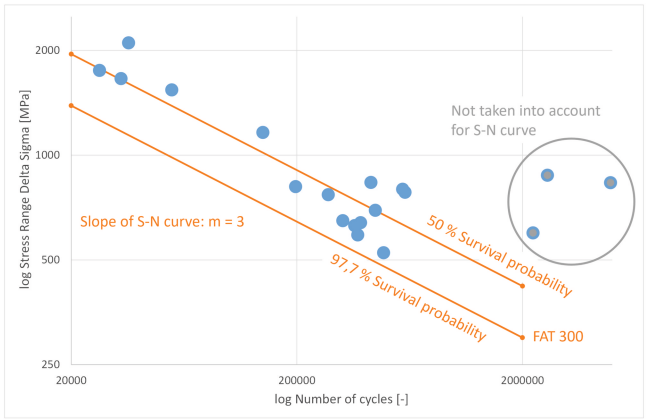

FIGURE 8 Results of the cruciform joints (19 samples): Stress range (first principal stress) of the finite element model plotted against the number of cracking cycles in the fatigue test. Preliminary proposed S–N curve for local stress based on the real geometry of the weld (FAT-class definition according to IIW, [1]).

BILD 8 Ergebnisse für die Kreuzproben (19 Prüflinge): Spannungsschwingbreite (1. Hauptspannung) der Finite-Elemente-Berechnung aufgetragen über Risslastspielzahl im Schwingversuch. Erster Vorschlag einer Wöhlerlinie für wahre Spannungen an Realgeometrien (FAT-Klassendefinition gemäß IIW, [1])

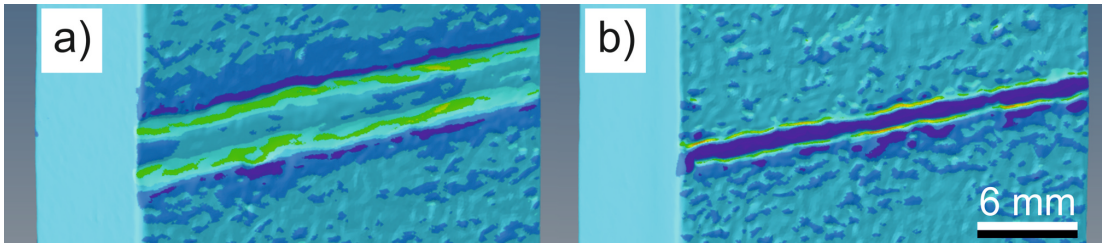

FIGURE 7 Result of the calculated laser-welded sample: Contour plot of the 1st main stress, a) transition at the weld toe, b) weld root.

BILD 7 Rechenergebnisse für die geschweißte Probe: Verteilung der 1. Hauptspannung, a) Nahtübergang, b) Nahtwurzel.

cycles at a R = 0.5, with a survival probability of 97.7%) a preliminary fatigue class for local stress based on the real geometry can be estimated to FAT 300.

6 | SUMMARY

A method has been shown to do the fatigue assessment of welded joints based on the real geometry of seam welds. Today it is possible to assess in detail a real weld geometry by using 3D-scanners. Based on these computerized data finite element models of the welds can be built, considering even small notches of the weld toe. Those notches are dominant for the fatigue behaviour of the weld seams. Based on several samples, which have been scanned, calculated with finite element methods and afterwards tested on a swing testing machine a fatigue class (i.e., SN-curve) for those models could be calculated. According to the IIW recommendations (stress range at 2 Mio. cycles, R = 0.5 and a survival probability of 97,7%) a local stress limit of 300 MPa (equal to FAT300) is proposed. Further investigations are planned.

ACKNOWLEDGEMENTS

Open Access funding enabled and organized by Projekt DEAL.

REFERENCES

1. A. Hobbacher, Recommendations for Fatigue Design of Welded Joints and Components, Springer, Berlin, **2016**.
2. W. Fricke, IIW Recommendations for the Fatigue Assessment of Welded Structures by Notch Stress Analysis, Woodhead Publishing, Cambridge, **2012**.
3. K. Letz, DVS Merkblatt 0905, DVS Media, Düsseldorf, Germany, **2017**.
4. R. Späth, presented at DVS Congress: Rostock, Germany, 16–17 September, **2019**, pp. 240–245.
5. E. Shams, AVIF A 268, Forschungsvereinigung Automobiltechnik e.V., FAT Schriftenreihe 250, **2013**.
6. R. Lang, G. Lehner, *Stahlbau* **2016**, *85*, 5, 336.
7. R. Lang, G. Lehner, *Stahlbau* **2016**, *85*, 6, 395.

How to cite this article: R. Späth, M. Steinebrunner, *Materialwiss. Werkstofftech.* **2023**, *54*, e202300020. https://doi.org/10.1002/mawe.202300020